Middle-East Journal of Scientific Research 24 (9): 2998-3009, 2016
ISSN 1990-9233

DOI: 10.5829/idosi.mejsr.2016.2998.3009

Performance Analysis of Wavelets on Multispectral Band Compression

[1]S. Thayammal and [2]D. Selvathi

[1]Department, AAA College of Engineering and Technology, Sivakasi -626 123, Tamil Nadu, India
[2]Department, Mepco Schlenk Engg. College, Sivakasi 625 005, Tamil Nadu, India

Abstract: The optimum wavelet is deployed in true color composite, false color composite (Near Infrared Composite) and Shortwave Infrared Composite of Landsat multispectral band image compression. Seven different kinds of wavelet families with various filter order are examined and optimum wavelets are identified from each wavelet family. The optimum decomposition level is determined by deploying with the identified optimum wavelets. The important properties of wavelets in compression and the image quality degradation during wavelet compression and decompression are discussed. The optimum wavelets and decomposition level are identified by reconstructed image quality and classification accuracy of reconstructed image. The reconstructed image quality is measured by both objective and subjective measures. The objective measures are peak signal to noise ratio (PSNR), compression ratio (CR), mean structural similarity index (MSSIM) and subjectively using perceived image quality. The classification accuracy is measured by Kappa coefficient. The simulation results provide good reference for applications developers, to choose optimum wavelet and decomposition level for their applications.

Key words: Multispectral band · Infrared composite · Wavelets · Similarity index · Kappa coefficient

INTRODUCTION

Landsat satellites have been providing multispectral images of the Earth continuously since the early 1970's. The applications of Landsat imagery are land and water management, global change research, oil and mineral exploration, agricultural yield forecasting, pollution monitoring, land surface change detection, and cartographic mapping. Multispectral images typically possess a high degree of spatial correlation [1]. The basic attribute for compression is correlated/redundant data in an image. Compression is achieved by removing one or more of three basic data redundancies: Spatial Redundancy, Spectral redundancy and Psycho-visual redundancy [2]. As a consequence, image compression can significantly reduce multispectral data volumes to more manageable size for storage and communication.

In the past two decades, various algorithms have been proposed for image compression. Most of them rely on transform coding because of its simplicity, better results and ease to implement. Among, discrete cosine transforms (DCT) [3] and discrete wavelet transform (DWT) are used in real time applications. The DCT is used in standard for compression of still images (e.g., JPEG). These standards usually do not provide satisfactory results for multispectral image [4]. In DCT based compression, the input image is subdivided into 8X8 sub-image and then DCT is applied. The transform itself does not give compression. The quantization of transformed coefficients will reduce the number of elements by making near-zero coefficients into zero. Further compression is obtained by source encoding. The block-based compression is the fundamental limitation of DCT based compression. It produces blocking artifacts in reconstructed image. The rate (bit rate or compression ratio) - distortion (reconstructed image quality) performance is depending upon size of sub image and frequency content of an image.

In past decades, much of the research activities in transform coding are focused on DWT. DWT has gained popularity [5-14], showing in this field the same interesting performance exhibited in other contexts. Wavelet becomes standard tool for image compression applications, because of its data reduction capability.

Corresponding Author: S. Thayammal, Department, AAA College of Engineering and Technology, Sivakasi -626 123, Tamil Nadu, India. E-mail: thaya.psr@gmail.com.

Unlike DCT, DWT is applied directly to the whole image and compression is achieved in transform itself. The research activities have been developed on analysis of wavelets for standard, medical, natural and artificial images [15-20]. These papers present in rate-distortion perspective alone and fail to justify in information preservation perspective through analysis or classification process after compression.

The performance of different wavelets namely, Daubechies, Coiflet, Symlet, biorthogonal, reverse biorthogonal and Discrete Meyer are analyzed with decomposition level 3 for multispectral images [21, 22]. The simulation results obtained using Landsat-5 multispectral image of forest and agricultural area and concluded that, the discrete Meyer wavelet produces better compression performance. Here they present both rate-distortion and information preservation perspectives. They do not consider about inter band redundancy of multispectral images which is one of the key factor for multispectral image compression. Hence their justification on wavelet analysis is not optimum for multispectral images.

To obtain optimum wavelet for multispectral image compression, principle component analysis (PCA) is used for spectral decorrelation. Spectral decorrelation via PCA results in rate distortion performance superior to that of spectral DWT [13]. In the proposed work, seven wavelets are selected depending upon their properties, which are suitable for spatial decorrelation. The seven selected wavelets are investigated with 3 different band (321,432) and (742) combinations of Landsat-7 multispectral images. This work has two primary objectives. First, investigate the impact of wavelets and its decomposition level to rate-distortion performance. Second, performance of this proposed work in terms of information preservation, i.e., in terms of the usefulness of the reconstructed image in analysis, such as detection and classification. Finally using observations of rate-distortion and data analysis performance, an optimum wavelet with decomposition level is determined.

The organization of this paper is as follows. Section II focuses on some important properties of wavelets and their usefulness in image compression. Section III presents performance measures of reconstructed image and compression method. The proposed methodology which is based on wavelet transform is presented in section IV. Section V provides simulation results and discussion of the proposed method and existing method. Finally conclusion and future work discussed in section VI.

Wavelet Transform: A wavelet function is a small wave, which must be oscillatory in some way to discriminate between different frequencies. Wavelets are defined by the wavelet function Ψ (t) (i.e. the mother wavelet) and scaling function φ (t) (also called father wavelet) in the time domain. As shown in Table I. orthonormality, vanishing order, regularity (smoothness) and symmetry are the desirable properties of wavelets which are important for image compression [23].

Wavelets with filters are associated with multi-resolution orthogonal or biorthogonal analyses; discrete transform and fast calculations using the Mallat algorithm are then possible [23]. Orthogonal wavelets preserve energy in the transform domain. The orthogonal property of wavelet that the MSE introduced by thresholding or quantization of transform coefficients is equal to MSE in the reconstructed image. Next the vanishing order is one of the important property of wavelet for image compression i, e it is responsible for compaction property of wavelets. Non smooth wavelet basis function introduces artificial discontinuities in quantization. This reflects that, the artifacts in reconstructed image. The classification of wavelet with filters listed in Table II.

Table I: desirable PROPERTIES OF Wavelets and their impact in image compression

S.No	Property	Uses
1	Orthogonal	Energy preservation
2	Number of zero moments of Ψ or φ (Vanishing order)	Compact support
3	Regularity (Degree of smoothness)	Reduce artifacts in reconstructed image.
4	Symmetry	Avoid dephasing

Table II: Classification of Wavelets with Filters

Wavelet with filters		
Wavelets with compact support		With non compact support
Orthogonal	Bi-orthogonal	Orthogonal
Daubechies (dB), Haar (haar), Symlets (sym), Coiflets (coif)	Biorthogonal (Bior), reverse biorthogonal (rbio)	Discrete approximation of the Meyer (Dmey)

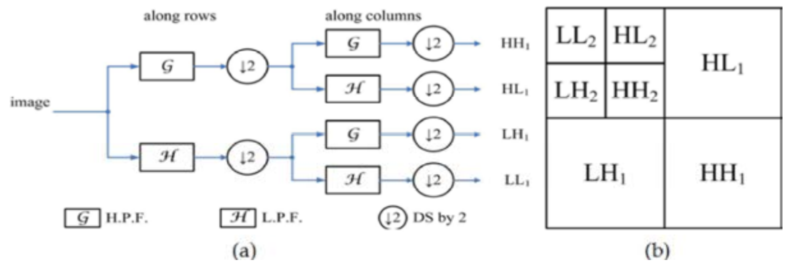

Fig. 1: a First level DWT decomposition and b) Second level DWT decomposition

The DWT uses multi resolution filter banks and special wavelet filters for the analysis and reconstruction of signals. Images are analyzed and synthesized by 2D filter banks. In images, the low frequencies, extracted by high scale wavelet functions and the high frequencies by low scale wavelet functions. The low-pass subband gives an approximation of the original image; the other bands contain detail information. The filter bank decomposition structure for DWT is as shown in Figure 1. The Figure 1.a. represents the first level decomposition and Figure.1.b. Represents the 2nd level decomposition of an input image.

Let $f(x, y) \in Z$, $1 \leq x \& y \leq N$ is an image with size $N \times N$, and the single level decomposition of an input image using wavelet transform is

$$T\{f(x,y)\} = LL_1(m,n), LH_1(m,n), HL_1(m,n), HH_1(m,n) \quad 1 \leq m,n \leq \frac{N}{2} \tag{1}$$

where

LL_1 - is the approximation of an input image.

LH_1 - is the horizontal detailed component of an input image.

HL_1 - is the vertical detailed component of an input image.

HH_1- is the diagonal detailed component of an input image.

And subscript represents decomposition level.

$LL_1(m,n) \cong f(x,y)$ With the compression ratio of 2. Here, the transform itself performs compression. The compression ratio increased by further decomposition of approximated LL1 (m, n) subimage. The second level decomposition of LL is given by

$$T\{LL_1(m,n)\} = \{LL_2(s,t), LH_2(s,t), HL_2(s,t), HH_1(s,t)\}$$

where $1 \leq s,t \leq \frac{N}{4}$ (2)

PERFORMANCE MEASURES

Reconstructed Image Quality Measures

Mean Square Error (MSE): The reconstructed image quality can be justified by objective and subjective measures. The objective measures are based on distortion measures. The reconstructed error is one of the standard objective distortion measures. The reconstructed error e(x, y) is the difference between the input image is represented as f(x, y) and reconstructed image is f'(x, y).

$$E(x, y) = f(x, y) - f'(x, y) \text{ x and y=1to N} \tag{3}$$

where NXN is the size of the image MSE refers to the average value of the square of the error between the original image and the reconstruction image.

$$MSE = \frac{1}{N^2}\sum_{x=1}^{N}\sum_{y=1}^{N}[f(x,y) - f'(x,y)]^2 \tag{4}$$

$$MSE = \frac{1}{N^2}\sum_{x=1}^{N}\sum_{y=1}^{N}e^2(x,y) \tag{5}$$

Peak Signal to Noise Ratio (PSNR): Peak Signal to Noise Ratio is derived from MSE and is given by

$$SSIM(x,y) = \frac{\left(2\mu_x\mu_y + c_1\right)(2\sigma_{xy} + c_1)}{\left(\mu_x^2\mu_y^2 + c_1\right)(\sigma_x^2 + \sigma_y^2 + c_2)} \tag{6}$$

Though PSNR is the most widely used objective image quality metric, its values do not perfectly correlate with a perceived visual quality due to the non-linear behavior of the human visual system.

Mean Structural Similarity Index Metric (MSSIM): The Structural Similarity Index Metric (SSIM) is a method for measuring the similarity between two images. SSIM is used to improve on traditional measures like Peak Signal-to-Noise Ratio (PSNR) and Mean Squared Error (MSE), which have proven to be inconsistent with human eye perception:

$$SSIM(x,y) = \frac{\left(2\mu_x\mu_y + c_1\right)(2\sigma_{xy} + c_1)}{\left(\mu_x^2\mu_y^2 + c_1\right)(\sigma_x^2 + \sigma_y^2 + c_2)} \tag{7}$$

μ_x = The average of x and μ_y the average of y
σ_x^2 = The variance of x and σ_y^2 the variance of y
σ_{xy} = The covariance of x and y
c_1 = $(k_1L)^2$, c_2 = $(k_2L)^2$ two variables to stabilize the division with weak denominator
L = The dynamic range of the pixel-values (typically this is 2^b-1, b number of bits/pixel)
k_1 = 0.01 and k_2 = 0.03 by default

Mean Structural Similarity Index Metric MSSIM is the better indication of image qualtiy and is defined as the mean value of SSIM. The MSSIM is determined by the following equation.

$$MSSIM = \frac{1}{N}\sum_{i=1}^{N} SSIM(xl, yl) \quad (8)$$

Classification Measure -Kappa Coefficient: When two binary variables are the measure of the same thing, Cohen's Kappa or Kappa Coefficient can be used as a measure of agreement between the two variables. If one variable is assumed to be the correct measure then Kappa coefficient will be the measure of correctness of the second one.

$$K = \frac{\Pr(a) - \Pr(e)}{1 - \Pr(e)} \quad (9)$$

where Pr (a) is the relative observed agreement among variables and Pr (e) is the hypothetical probability of chance agreement, using the observed data to calculate the probabilities of each variable randomly saying each category. If the variables are in complete agreement then K = 1. If there is no agreement among the variables then K = 0.

Image Compression Using Wavelet Transform: The algorithm steps of proposed methodology are as follows:

- Read individual multispectral band imagery which are in grey level values $f_i(x, y)$, and size of an image is 7550 × 7581.
- Combine an individual band images into single multispectral imagery using layer stacking in ENVI tool

$$g_{mb}(x, y) = stack\{f_i(x, y)\} \quad (10)$$

where
$i = 3,2,1\ (R = 3, G = 2, B = 1)$ for true color composite
$i = 4,3,2\ (R = 4, G = 3, B = 2)$ for Near Infrared (NIR) Composite
$i = 7,4,2\ (R = 7, G = 4, B = 2)$ for Shortwave Infrared *composite*

- The spectral correlation of gmb(x, y) is removed and difference between bands are enhanced by spectral decorrelation stretching operation using ENVI tool. Here enhancement by stretching does not introduce redundancy in the enhanced decorrelated image gmb.SDS(x,y).
- From ENVI package, Export multispectral image gmb, SDS(x, y) as an external image file.
- From MATLAB, import an image gmb, SDS(x, y) and extract each band separately as gb (x, y).
- By the following steps, the optimum wavelets are chosen by using rate-distortion performance of the compression of individual band image.
    - Wavelet decomposition of an input image gb (x, y) is

$$g_{bw}(m, n) = W\{g_b(x, y)\} \quad \forall x, y, m, n \in Z \text{ and } 1 \le m, n = \le \frac{N}{2} \quad (11)$$

where
W= wavelet transform
$g_{bW} = \{g_a, g_h, g_v, g_d\}$
g_a is the approximation of an input image
g_h is the detailed component in horizontal direction.
g_v is the detailed component in vertical direction.
g_d is the detailed component in diagonal direction.

- Determine adaptive threshold value of g_a and performed adaptive thresholding of approximated wavelet coefficients.

$$T_{ADA} = select\_thresh(g_a) \quad (12)$$

$$g_{aT} = T_{ADA}(g_a) \quad (13)$$

- Encoding of thresholded values is performed using Set Partitioning in Hierarchical Trees (SPIHT) technique, which is suitable for wavelet coefficients.

$$f_{a(comp)} = SPIHT(f_{aT}) \quad (14)$$

- Compression ratio (CR) is calculated by using the ratio of number of bytes required (Mi) to represent an input image and number of bytes required to represent SPIHT encoding stream (Mo).

$$\text{Compression Ratio (CR)} = \frac{M_i}{M_o} \quad (15)$$

- SPIHT decoding of encoded bit stream is performed.

$$f_{a(decomp)} = \text{SPIHT\_decode}(f_{a(comp)}) \quad (16)$$

- The original image is reconstructed by applying inverse discrete wavelet transform to decoded or decompressed Image.

$$f_{a(rec)} = \{\text{IDWT}(f_{a(decomp)})\} \quad (17)$$

- The various objective measures like Peak Signal to Noise Ratio (PSNR), Structural Similarity Index (MSSIM) are calculated using input and reconstructed images.
- From rate-distortion performance, optimum wavelets are chosen.
- Optimum wavelets with various decomposition level (DL=2 to 10) are deployed and few number of decomposition levels are chosen from rate-distortion performance.
- The reconstructed images using optimum wavelets with decomposition level are export to ENVI tool.
- Read an individual reconstructed band of each composite image and combine them with 321, 432 and 742 respective composite bands.
- The unsupervised classification technique like k-means algorithm is applied to the composite bands with 2 numbers of classes (water body and non water body).
- With the help of post classification tool, the classification accuracy is determined by Kappa coefficient.
- Application specific optimum wavelet with decomposition level is determined using rate - distortion performance and effective reconstruction of image for analysis and further classification.

Simulation Results and Discussions: The simulation results are obtained for Landsat ETM+ image with 8 bit radiometric resolution representing cud lore district, Tamil nadu (path/row : 142/52). Five equal resolution bands (band 1,2,3,4 and 7) are used to produce three multispectral composite bands, 321, 432 and 742. An area of 512x512 pixels is taken as a test image which exhibits both water and non -water body area. The simulation results present to assess the performance of the proposed technique, also compared with reference techniques given in the literature [17, 18, 22].

The spectral decorrelation stretching method is used to eliminate inter band correlation and also highlight the difference between inter bands. The individual band from 3, 2 and 1 (true color composite 321), band 4,3 and 2(false color composite) and band 7,4 and 2 (from short wave infrared 742) is compressed using seven different wavelets of various filter order N: Haar, discrete meyer wavelet with N (dmeyN)= 1, 2, 4, 5, 6, 8, 10, 15, 16, 32, 45, biorthogonal wavelet with Nr,Nd (biorNr.Nd) = (1,1), (1,3), (1,5), (2,2), (2,4), (2,6), (2,8), (3,1), (3,3), (3,5), (3,7), (3,9), (4,4), (5,5), and (6,8), coiflet wavelet with N (coifN) = 1, 2, 3, 4 and 5, daubechies wavelet with N (dbN)=1, 2, 4, 5, 6, 8, 10, 15, 16, 32 and 45 symlet wavelet with N (symN) = 1,2,3,5,8,13,18,23,28 and 32 and reverse biorthogonal wavelet with Nr,Nd (rbioNr.Nd) = (1,1), (1,3), (1,5), (2,2), (2,4), (2,6), (2,8), (3,1), (3,3), (3,5), (3,7), (3,9), (4,4), (5,5), and (6,8). The optimum wavelet with filter order is chosen from each family using PSNR, CR and MSSIM values.

Analysis of Wavelet Families: Table III, IV and V show the compression ratio, PSNR and MSSIM on a per band basis for three composite bands using seven different wavelet families with single decomposition level. There is tradeoff between compression ratio and PSNR. In a few steps, the choice of an optimum wavelet is determined for multispectral image compression. For each wavelet family, the optimal filter order is determined.

Among seven wavelet families, the Haar and dmey chosen for next step analysis, because they don't have filter order variation. In biorthogonal wavelet family, for all the three composite bands 321,432 and 742, the PSNR values are low comparing other wavelet families. Because biorthogonal wavelet family does not possess orthogonal property except bior2.2, which possesses near orthogonal property. Though bior3.1 produces high compression ratio, bior2.2 is chosen by considering reconstructed image quality (PSNR), complexity in (bior3.1) higher filter order.

In coiflet wavelet family, all wavelets produce approximately same results (CR ~40 and PSNR~ 30dB). Hence coif1 is chosen by considering complexity in higher filter order. Among Daubechies family, Db1 produces high CR and PSNR. The regularity (responsible for image quality) and vanishing order (responsible for compression ratio) are decayed with increasing filter order of Db family, so that the artifacts introduced in reconstructed image and compression ratio is decreased. Hence the PSNR reduced with increasing filter order. Here Db1 is chosen by considering PSNR and complexity in higher filter order. As Db family, among in symlet family, sym1 is chosen which produces high CR and PSNR. For higher filter order (sym33 to sym45), the simulation does not executed which requires large volume of memory. For reverse biorthogonal wavelet family, the compression ratio decreases with increasing filter order up to rbio3.1, after that CR is increased. The rbio1.1 produces optimum CR and PSNR.

Table III: Rate - Distortion Performance of True Color Composite Band Compression Using Various Wavelet Families

S.No	Waveletfamily	WaveletFilter order	Band3 CR	Band3 PSNR	Band3 MSSIM	Band2 CR	Band2 PSNR	Band2 MSSIM	Band1 CR	Band1 PSNR	Band1 MSSIM
1	Haar		41.3387	31.5639	0.9708	39.7465	31.5845	0.9716	40.1554	30.9497	0.9707
2	dmey		40.5239	31.0983	0.9650	39.7579	31.4496	0.9691	40.7191	30.4246	0.9663
3	Biorthogonal	bior1.1	41.3387	31.5639	0.9708	39.7465	31.5845	0.9716	40.1554	30.9497	0.9707
		bior1.3	40.4682	31.3655	0.9695	39.3527	31.4854	0.9709	40.4528	30.5180	0.9679
		bior1.5	40.7060	30.9132	0.9664	39.8695	31.0418	0.9678	40.6132	30.1769	0.9655
		bior2.2	43.0293	29.9439	0.9607	42.2552	30.0093	0.9591	42.9170	29.2629	0.9594
		bior2.4	42.9157	30.0165	0.9610	42.3913	30.1083	0.9598	42.9386	29.3868	0.9603
		bior2.6	42.9830	29.9131	0.9600	42.4509	30.0652	0.9594	43.1575	29.2476	0.9591
		bior2.8	42.9627	29.8211	0.9591	42.6090	29.9472	0.9583	43.1678	29.1636	0.9583
		bior3.1	44.7353	26.0266	0.9173	44.1562	25.9066	0.9033	44.4132	25.3905	0.9150
		bior3.3	44.2167	27.6384	0.9388	44.0639	27.5312	0.9299	44.4519	26.9370	0.9361
		bior3.5	44.1931	27.9508	0.9422	44.0488	27.8959	0.9347	44.4015	27.2855	0.9399
		bior3.7	44.1553	28.0439	0.9430	44.0302	28.0080	0.9361	44.4101	27.3768	0.9408
		bior3.9	44.2179	28.0298	0.9427	44.0110	28.0442	0.9365	44.4874	27.3771	0.9407
		bior4.4	40.8968	31.2198	0.9687	40.1361	31.3642	0.9695	40.8750	30.5511	0.9683
		bior5.5	38.2290	31.8047	0.9719	36.9959	32.1227	0.9741	37.9809	31.1596	0.9720
		bior6.8	40.9765	31.1613	0.9680	40.5073	31.3020	0.9689	41.3679	30.3866	0.9671
4	Coiflet	coif1	40.5685	31.3663	0.9700	39.5751	31.6380	0.9714	40.2680	30.7506	0.9697
		coif2	40.6688	31.3233	0.9692	39.7587	31.6172	0.9711	40.6673	30.6716	0.9691
		coif3	40.6146	31.2991	0.9686	39.7935	31.6005	0.9709	40.7430	30.6153	0.9685
		coif4	40.5662	31.2888	0.9683	39.8038	31.5783	0.9707	40.8156	30.5581	0.9680
		coif5	40.6152	31.2399	0.9676	39.8018	31.5648	0.9705	40.9263	30.4947	0.9675
5	Daubchies	db1	41.3387	31.5639	0.9708	39.7465	31.5845	0.9716	40.1554	30.9497	0.9707
		db2	40.6032	31.4192	0.9700	39.4537	31.6814	0.9716	40.3004	30.7054	0.9694
		db4	40.9006	31.2711	0.9682	40.0300	31.5630	0.9704	40.9438	30.6060	0.9683
		db5	40.7004	31.2293	0.9677	39.7822	31.5852	0.9704	40.7149	30.6132	0.9680
		db6	40.5635	31.1541	0.9664	39.8266	31.4968	0.9697	40.7833	30.4583	0.9668
		db8	40.3772	31.1138	0.9654	39.5466	31.4288	0.9689	40.5803	30.3543	0.9656
		db10	40.3418	31.0124	0.9642	39.7077	31.3433	0.9681	40.7095	30.2633	0.9649
		db15	40.1996	30.9212	0.9622	39.4527	31.3180	0.9678	40.5566	30.1732	0.9640
		db16	40.5063	30.7746	0.9611	39.6059	31.2263	0.9671	40.7528	30.0321	0.9628
		db32	40.5310	30.4660	0.9567	39.3188	31.0914	0.9664	40.6221	29.8234	0.9614
		db45	40.4039	30.4523	0.9557	39.4886	30.9784	0.9657	40.5153	29.7585	0.9609
6	Symlet	Sym1	41.3387	31.5639	0.9708	39.7465	31.5845	0.9716	40.1554	30.9497	0.9707
		sym2	40.6032	31.4192	0.9700	39.4537	31.6814	0.9716	40.3004	30.7054	0.9694
		sym3	40.6710	31.4014	0.9695	39.8620	31.5793	0.9706	40.6458	30.6766	0.9689
		sym5	40.6143	31.3172	0.9689	39.7940	31.5565	0.9705	40.6912	30.6235	0.9686
		sym8	40.4910	31.3119	0.9684	39.7255	31.5699	0.9705	40.5919	30.6151	0.9683
		sym13	40.4412	31.2482	0.9674	39.7113	31.5358	0.9700	40.6873	30.4975	0.9673
		sym18	40.4517	31.2202	0.9666	39.7630	31.4958	0.9696	40.7559	30.4447	0.9668
		sym23	40.7329	31.1079	0.9651	39.8915	31.4860	0.9693	40.8131	30.4075	0.9659
		sym28	40.4962	31.1565	0.9657	39.8176	31.4857	0.9693	40.6055	30.4956	0.9668
		sym32	40.4032	31.1565	0.9651	39.7085	31.4763	0.9692	40.7593	30.3914	0.9661
7	Reverse biorthogonal	rbio1.1	41.3387	31.5639	0.9708	39.7465	31.5845	0.9716	40.1554	30.9497	0.9707
		rbio1.3	40.9215	31.4141	0.9704	39.2671	31.6001	0.9715	40.1997	30.6895	0.9696
		rbio1.5	41.0137	31.0794	0.9679	39.4996	31.2406	0.9689	40.1775	30.4206	0.9679
		rbio2.2	37.0782	31.6241	0.9715	35.5444	32.0854	0.9743	36.3222	30.9794	0.9710
		rbio2.4	37.5444	31.8194	0.9724	36.0322	32.1386	0.9745	37.0821	31.0884	0.9719
		rbio2.6	37.8092	31.6747	0.9713	35.8546	32.1840	0.9747	37.1001	31.0452	0.9715
		rbio2.8	37.4688	31.7407	0.9714	35.8984	32.0905	0.9741	36.9734	31.0149	0.9713
		rbio3.1	32.5319	29.5324	0.9561	30.6500	30.2476	0.9622	32.0925	28.7091	0.9536
		rbio3.3	34.4024	30.6884	0.9657	32.5230	31.3943	0.9702	33.9783	29.9625	0.9648
		rbio3.5	34.6116	31.0140	0.9677	32.8405	31.6274	0.9716	34.1671	30.2839	0.9671
		rbio3.7	34.6109	31.1056	0.9677	32.8178	31.7422	0.9722	34.1829	30.3870	0.9677
		rbio3.9	34.5874	31.1140	0.9678	32.7618	31.7805	0.9724	34.2577	30.3921	0.9677
		rbio4.4	40.3491	31.1496	0.9678	39.5455	31.4189	0.9698	40.3095	30.4641	0.9675
		rbio5.5	42.8429	30.0078	0.9597	42.2322	30.2388	0.9605	43.1475	29.2662	0.9585
		rbio6.8	39.8972	31.4219	0.9692	39.2071	31.6796	0.9714	40.1286	30.6639	0.9687

Table IV: Rate - Distortion Performance of False Color Composite Band Compression Using Various Wavelet Families

			Band4			Band3			Band2		
S.No	Waveletfamily	WaveletFilter order	CR	PSNR	MSSIM	CR	PSNR	MSSIM	CR	PSNR	MSSIM
1	Haar		42.2115	39.9209	0.9641	40.8134	30.1888	0.9672	39.8849	31.8728	0.9719
2	dmey		40.8769	40.0467	0.9648	41.0683	29.8784	0.9648	40.2882	31.5965	0.9695
3	Biorthogonal	bior1.1	42.2115	39.9209	0.9641	40.8134	30.1888	0.9672	39.8849	31.8728	0.9719
		bior1.3	41.0278	39.8773	0.9638	40.6973	29.8334	0.9646	40.0438	31.5393	0.9698
		bior1.5	41.0385	39.5325	0.9612	40.9405	29.4830	0.9620	40.1017	31.2610	0.9679
		bior2.2	43.5603	38.8902	0.9608	43.2471	28.6553	0.9568	42.7292	30.2613	0.9608
		bior2.4	43.5033	38.8614	0.9603	43.2851	28.7510	0.9573	42.6942	30.4130	0.9618
		bior2.6	43.2973	38.8490	0.9601	43.4466	28.6453	0.9562	42.8858	30.3029	0.9608
		bior2.8	43.5043	38.6762	0.9589	43.4903	28.5617	0.9555	42.9192	30.2127	0.9601
		bior3.1	45.8054	35.2527	0.9370	44.8977	24.9360	0.9138	44.3133	26.3652	0.9142
		bior3.3	45.2710	36.7416	0.9492	44.8652	26.4080	0.9342	44.3058	27.9289	0.9365
		bior3.5	45.0871	37.0544	0.9513	44.8691	26.7415	0.9379	44.3200	28.2701	0.9406
		bior3.7	45.0570	37.1338	0.9515	44.8644	26.8592	0.9393	44.3233	28.3704	0.9416
		bior3.9	45.0534	37.1543	0.9515	44.9003	26.8737	0.9394	44.3062	28.3935	0.9419
		bior4.4	41.3266	40.0324	0.9665	41.2504	29.9201	0.9659	40.5322	31.6311	0.9704
		bior5.5	39.3003	40.2780	0.9674	38.5450	30.4764	0.9696	37.6965	32.2686	0.9742
		bior6.8	41.6100	39.8662	0.9653	41.6434	29.8132	0.9650	41.0027	31.5131	0.9695
4	Coiflet	coif1	40.5437	40.2117	0.9666	40.6323	29.9936	0.9660	40.0393	31.8382	0.9716
		coif2	40.9092	40.0874	0.9660	40.9804	30.0318	0.9664	40.2695	31.8134	0.9714
		coif3	40.8158	40.1223	0.9663	41.1745	29.9671	0.9659	40.3215	31.7884	0.9712
		coif4	41.0754	39.9911	0.9653	41.1249	29.9663	0.9658	40.3523	31.7497	0.9708
		coif5	40.9246	40.0447	0.9656	41.2308	29.9124	0.9653	40.3536	31.7297	0.9707
5	Daubchies	db1	42.2115	39.9209	0.9641	40.8134	30.1888	0.9672	39.8849	31.8728	0.9719
		db2	40.8310	40.1214	0.9660	40.4363	30.0719	0.9666	40.0676	31.8051	0.9715
		db4	41.1391	40.0267	0.9653	41.0183	30.0159	0.9662	40.4455	31.7675	0.9711
		db5	40.9246	39.9562	0.9647	41.0939	29.9089	0.9652	40.4874	31.6760	0.9703
		db6	40.9389	39.8204	0.9637	41.0556	29.8401	0.9647	40.3939	31.6250	0.9697
		db8	40.9721	39.6523	0.9622	40.9728	29.7465	0.9639	40.1282	31.5456	0.9690
		db10	40.8690	39.5907	0.9614	41.0192	29.6604	0.9629	40.2937	31.4565	0.9684
		db15	40.7428	39.4472	0.9599	41.0305	29.5407	0.9620	40.2641	31.3388	0.9673
		db16	40.8886	39.3258	0.9586	41.0020	29.5096	0.9618	40.1724	31.3521	0.9674
		db32	40.9893	39.0307	0.9553	41.1778	29.2035	0.9597	40.1793	31.1187	0.9660
		db45	41.1400	38.9460	0.9542	41.1133	29.1970	0.9597	40.3156	30.9784	0.9652
6	Symlet	Sym1	42.2115	39.9209	0.9641	40.8134	30.1888	0.9672	39.8849	31.8728	0.9719
		sym2	40.8310	40.1214	0.9660	40.4363	30.0719	0.9666	40.0676	31.8051	0.9715
		sym3	41.2565	40.0116	0.9656	41.0064	30.0015	0.9660	40.2590	31.8028	0.9713
		sym5	41.0155	39.9791	0.9652	40.9101	29.9785	0.9662	40.2467	31.7405	0.9709
		sym8	40.8471	40.0190	0.9655	40.9801	29.9843	0.9660	40.3862	31.6985	0.9705
		sym13	41.0542	39.8751	0.9640	40.8934	29.9354	0.9654	40.3539	31.6517	0.9700
		sym18	40.8697	39.9388	0.9647	40.9837	29.9365	0.9653	40.4141	31.6192	0.9697
		sym23	40.8995	39.8621	0.9634	41.1958	29.8590	0.9645	40.5223	31.5912	0.9694
		sym28	41.0855	39.8327	0.9633	41.0821	29.8707	0.9646	40.4182	31.5821	0.9694
		sym32	40.8446	39.9272	0.9640	40.9532	29.9166	0.9649	40.3866	31.5621	0.9692
7	Reverse biorthogonal	rbio1.1	42.2115	39.9209	0.9641	40.8134	30.1888	0.9672	39.8849	31.8728	0.9719
		rbio1.3	41.2415	40.1975	0.9675	40.6785	30.0761	0.9669	39.7989	31.7546	0.9715
		rbio1.5	41.5902	39.8207	0.9649	40.7171	29.7936	0.9649	39.7663	31.5146	0.9699
		rbio2.2	38.5903	39.8178	0.9627	36.6929	30.2061	0.9669	36.1566	32.1356	0.9735
		rbio2.4	39.4338	39.8822	0.9639	37.5348	30.3330	0.9684	36.6354	32.2801	0.9744
		rbio2.6	39.1312	40.0296	0.9650	37.6413	30.3021	0.9682	36.6492	32.2511	0.9742
		rbio2.8	39.4987	39.8117	0.9637	37.5369	30.2860	0.9681	36.5365	32.2184	0.9739
		rbio3.1	36.4790	36.7634	0.9321	32.7564	27.7031	0.9451	31.4320	29.9916	0.9585
		rbio3.3	37.8345	38.2363	0.9518	34.3968	29.1553	0.9605	33.5400	31.1573	0.9679
		rbio3.5	38.0272	38.6315	0.9557	34.8053	29.4147	0.9628	33.7216	31.5167	0.9703
		rbio3.7	38.0279	38.7718	0.9568	34.8718	29.5360	0.9636	33.7503	31.6129	0.9708
		rbio3.9	38.0780	38.7892	0.9571	34.9057	29.5658	0.9638	33.7455	31.6219	0.9708
		rbio4.4	40.8861	39.7044	0.9626	40.5325	29.7984	0.9646	39.9471	31.6266	0.9701
		rbio5.5	42.9680	38.7306	0.9571	43.3611	28.6404	0.9556	42.7078	30.4095	0.9613
		rbio6.8	40.6178	39.9436	0.9644	40.3190	30.0730	0.9665	39.7498	31.8323	0.9714

Table V: Rate - Distortion Performance of Short Wave Infrared Band Compression Using Various Wavelet Families

			Band7			Band4			Band2		
S.No	Waveletfamily	WaveletFilter order	CR	PSNR	MSSIM	CR	PSNR	MSSIM	CR	PSNR	MSSIM
1	Haar		44.1154	37.9380	0.9701	40.9218	39.7109	0.9611	40.5434	34.7550	0.9688
2	dmey		40.4318	37.3537	0.9608	40.6695	39.8209	0.9622	41.3428	34.3261	0.9671
3	Biorthogonal	bior1.1	44.1154	37.9380	0.9701	40.9218	39.7109	0.9611	40.5434	34.7550	0.9688
		bior1.3	41.6336	37.9057	0.9698	40.4832	39.5726	0.9599	40.9850	34.2634	0.9655
		bior1.5	41.8850	37.2562	0.9648	41.1690	39.0464	0.9556	41.4745	33.8018	0.9620
		bior2.2	43.6103	36.4504	0.9599	43.0075	38.5417	0.9557	43.4544	33.1715	0.9590
		bior2.4	43.2053	36.4223	0.9592	43.2470	38.5046	0.9549	43.6442	33.1865	0.9589
		bior2.6	42.9921	36.3565	0.9583	43.1505	38.4942	0.9549	43.6666	33.1326	0.9584
		bior2.8	43.1725	36.1434	0.9563	43.3278	38.3585	0.9539	43.8167	33.0073	0.9573
		bior3.1	45.5242	32.5259	0.9227	45.0794	34.8770	0.9311	45.0378	29.5111	0.9217
		bior3.3	44.8819	33.9246	0.9381	45.1309	36.2872	0.9428	45.0634	30.9801	0.9390
		bior3.5	44.6635	34.2205	0.9410	45.0672	36.6261	0.9452	45.1861	31.2620	0.9419
		bior3.7	44.5886	34.2850	0.9412	44.9967	36.7323	0.9459	45.1669	31.3582	0.9428
		bior3.9	44.5874	34.2730	0.9407	45.0189	36.7365	0.9458	45.2371	31.3482	0.9426
		bior4.4	41.0237	37.6213	0.9675	41.2371	39.5997	0.9616	41.6095	34.3291	0.9677
		bior5.5	38.5876	38.0141	0.9692	39.2761	39.8461	0.9630	38.9087	34.7742	0.9704
		bior6.8	41.0859	37.3975	0.9653	41.4723	39.5293	0.9610	41.9066	34.2291	0.9667
4	Coiflet	coif1	40.7859	37.9056	0.9694	40.2954	39.7498	0.9615	40.7536	34.5013	0.9679
		coif2	40.7088	37.7056	0.9676	40.9529	39.6559	0.9613	41.2332	34.4579	0.9681
		coif3	40.4578	37.6650	0.9668	40.7538	39.7490	0.9620	41.3406	34.4032	0.9677
		coif4	40.5515	37.5290	0.9652	41.0004	39.6400	0.9612	41.2416	34.4209	0.9679
		coif5	40.4215	37.5211	0.9648	40.7891	39.7317	0.9618	41.4774	34.3256	0.9672
5	Daubchies	db1	44.1154	37.9380	0.9701	40.9218	39.7109	0.9611	40.5434	34.7550	0.9688
		db2	41.3504	37.8628	0.9689	40.4457	39.6721	0.9607	40.6395	34.4890	0.9677
		db4	41.0027	37.4588	0.9652	40.8674	39.6321	0.9608	41.3481	34.4068	0.9676
		db5	40.5107	37.3968	0.9637	40.6331	39.6346	0.9607	41.2670	34.3470	0.9670
		db6	40.6666	37.1246	0.9613	40.7334	39.4811	0.9593	41.3988	34.2020	0.9661
		db8	40.5315	36.9513	0.9588	40.5883	39.4054	0.9585	41.2793	34.1333	0.9655
		db10	40.4151	36.7512	0.9560	40.8423	39.2689	0.9580	41.3667	33.9774	0.9644
		db15	40.2088	36.5107	0.9524	40.7545	39.1507	0.9566	41.2483	33.8912	0.9641
		db16	40.2783	36.4215	0.9509	40.8457	39.0923	0.9560	41.4724	33.8298	0.9635
		db32	40.5089	35.7899	0.9418	40.7993	38.9202	0.9543	41.2279	33.6225	0.9622
		db45	40.7872	35.5046	0.9377	40.8967	38.8714	0.9538	41.4228	33.4996	0.9615
6	Symlet	Sym1	44.1154	37.9380	0.9701	40.9218	39.7109	0.9611	40.5434	34.7550	0.9688
		sym2	41.3504	37.8628	0.9689	40.4457	39.6721	0.9607	40.6395	34.4890	0.9677
		sym3	40.9981	37.6720	0.9671	40.8870	39.6247	0.9608	41.2847	34.3964	0.9674
		sym5	40.7496	37.4903	0.9657	40.7367	39.6559	0.9612	41.3506	34.3582	0.9673
		sym8	40.7180	37.3988	0.9645	40.9128	39.6282	0.9609	41.2580	34.3909	0.9677
		sym13	40.4102	37.3220	0.9628	40.8756	39.5784	0.9605	41.4137	34.2622	0.9667
		sym18	40.5577	37.2135	0.9613	40.8267	39.6263	0.9609	41.4443	34.2526	0.9667
		sym23	40.5297	37.1104	0.9591	40.6973	39.5948	0.9603	41.4216	34.2479	0.9664
		sym28	40.3735	37.2855	0.9608	40.7188	39.6535	0.9610	41.4320	34.2427	0.9664
		sym32	40.4348	37.2586	0.9603	40.6913	39.6811	0.9611	41.4661	34.2364	0.9664
7	Reverse biorthogonal	rbio1.1	44.1154	37.9380	0.9701	40.9218	39.7109	0.9611	40.5434	34.7550	0.9688
		rbio1.3	42.0757	38.0364	0.9707	40.5208	39.7365	0.9623	40.5685	34.5766	0.9692
		rbio1.5	42.4035	37.5450	0.9667	40.5958	39.4813	0.9607	40.7016	34.2671	0.9673
		rbio2.2	38.6902	37.9150	0.9681	38.1276	39.3425	0.9573	37.1090	34.4666	0.9671
		rbio2.4	39.4234	37.9148	0.9685	38.8229	39.5053	0.9595	38.1727	34.5586	0.9686
		rbio2.6	39.2817	37.9175	0.9681	38.7703	39.5723	0.9601	37.9800	34.6355	0.9694
		rbio2.8	39.3419	37.7874	0.9670	38.8835	39.4841	0.9595	38.1148	34.5282	0.9686
		rbio3.1	36.4809	34.9179	0.9398	36.0297	36.4185	0.9270	33.4941	31.5530	0.9382
		rbio3.3	37.3656	36.3057	0.9555	37.3027	37.9826	0.9478	35.4668	33.0970	0.9574
		rbio3.5	37.4305	36.6288	0.9579	37.5369	38.3397	0.9516	35.7082	33.4703	0.9609
		rbio3.7	37.3918	36.6763	0.9582	37.5381	38.4671	0.9531	35.6854	33.6365	0.9623
		rbio3.9	37.3738	36.6556	0.9577	37.5959	38.4792	0.9532	35.6981	33.6660	0.9626
		rbio4.4	40.6587	37.4473	0.9653	40.6483	39.3033	0.9579	41.1694	34.0758	0.9651
		rbio5.5	42.6520	36.2599	0.9561	42.6781	38.4427	0.9524	43.5468	33.0588	0.9571
		rbio6.8	40.0737	37.5912	0.9655	40.5637	39.5734	0.9602	40.7226	34.4121	0.9676

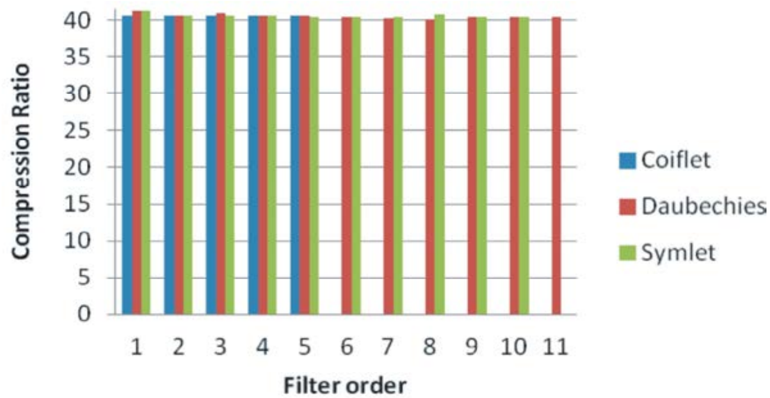

Fig. 2: Analysis of compression ratio using Coiflet, Daubechies and symlet wavelet family from Table III

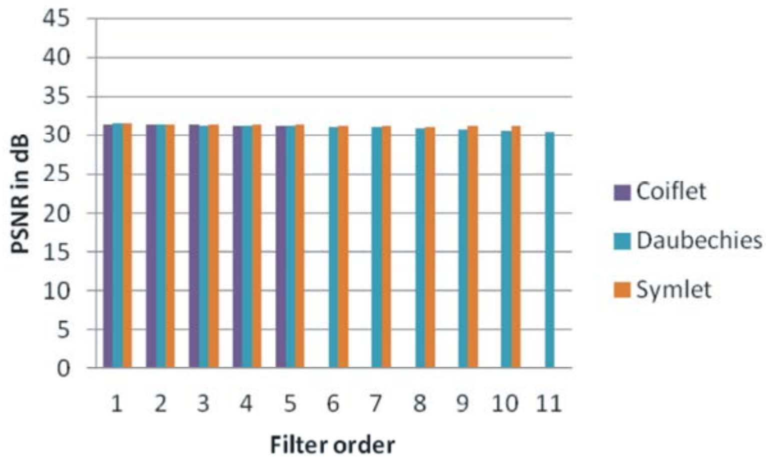

Fig. 3: Analysis of PSNR using Coiflet, Daubechies and symlet wavelet family from Table III

For all composite bands, the Coiflet (except coif1), Daubechies (except Db1) and symlet (except Db1) wavelet produce almost same response. Fig. 2 and 3 depict the compression ratio and PSNR values produced by the families of Coiflet, Daubechies and Symlet for band 3 of true color composite 321. The selected haar wavelet, db1 from daubechies family, sym1 from symlet family and rbio1.1 from reverse biorthogonal family produce same results for all composite bands. Hence haar wavelet is chosen among four different wavelet families. The analysis of these simulation results reveals that Haar, bior2.2 and coif1 are produced better performance than other wavelets for all composite bands, also these three wavelets are chosen for next step decomposition level analysis.

Analysis of Decomposition Level: The Db2, dmey and rbio1.3 wavelets are proven as optimum wavelet by different existing algorithms. Hence for comparative analysis, already chosen wavelets by the proposed technique are combined with these three wavelets for next stage decomposition level analysis. The six wavelets nameley haar, bior2.2, coif1, dmey, Db2 and rbio1.3 are analysed with different decomposition level (DL=1 to 10). From Fig 5a it is observed that, the compression ratio is increased upto DL=3 and it maintains constant value. The PSNR reduced with increasing decomposition level upto DL=3, it also maintains constant values as shown in Fig 5.b The detail components are eliminated with increasing decomposition level. Hence the PSNR and MSSIM are reduced.

Comparative Analysis with Existing Technique: The optimum wavelet is chosen by kappa coefficient of classification measure and output of classified image. The kappa coefficient of classified image is obtained for six wavelets with decomposition level 1,2 and 3 are listed in Table VI which proves that, though Haar wavelet produces high Kappa coefficient for 3 composite bands with various decomposition level (DL=1,2 & 3).

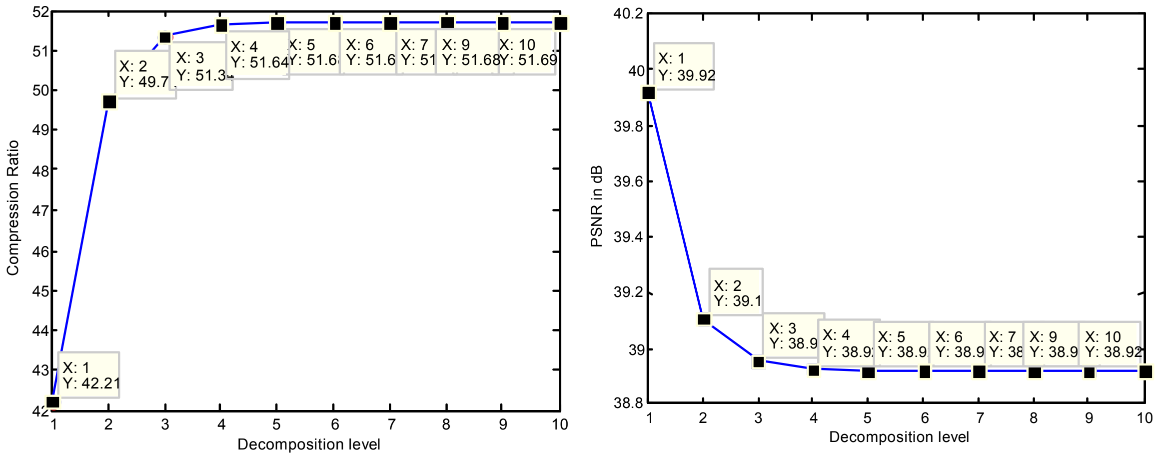

Fig. 4: Analysis of Rate - Distortion performance with decomposition level (band 4 of false color composite 432 is compressed by haar wavelet)

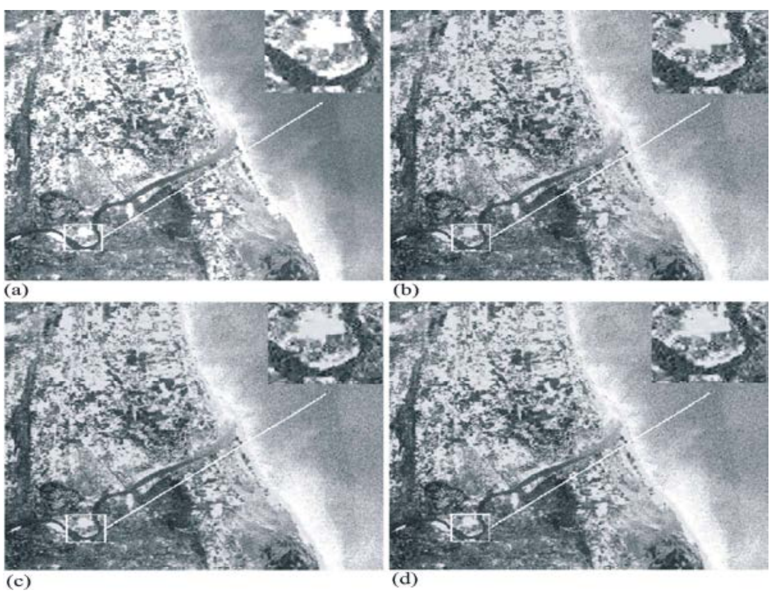

Fig. 5: (a) Input Image (b) Input image compressed by haar (c) bior2.2 and (d) rbio1.3

Table VI: Analysis of Classification Measure - Kappa Coefficient

Decompositionlevel	Bandcomposite	Haar[10]	Dmey[12]	db2[11]	bior2.2	coif1	rbio1.3[11]
1	Band321	0.9290	0.9262	0.9257	0.9258	0.9261	0.9257
	Band432	0.8728	0.8702	0.8682	0.8663	0.8681	0.8698
	Band742	0.8891	0.8851	0.8847	0.8847	0.8852	0.8847
2	Band321	0.8066	0.8066	0.8069	0.8074	0.8069	0.8058
	Band432	0.869	0.8679	0.8598	0.8568	0.8592	0.8656
	Band742	0.8806	0.8795	0.8776	0.8776	0.879	0.8776
3	Band321	0.8025	0.8025	0.8036	0.8039	0.8036	0.8016
	Band432	0.866	0.8657	0.8589	0.8578	0.8583	0.8658
	Band742	0.8786	0.8782	0.878	0.878	0.8784	0.878

Fig. 5 compares the visual quality of test image compressed by optimal wavelet functions (haar, bior2.2 and rbio 1.3) of proposed algorithm with three level decomposition. Compare figure c, in figure b and d, the fine details are lost and region borders are showing peaks of error. The reconstructed image from all composite

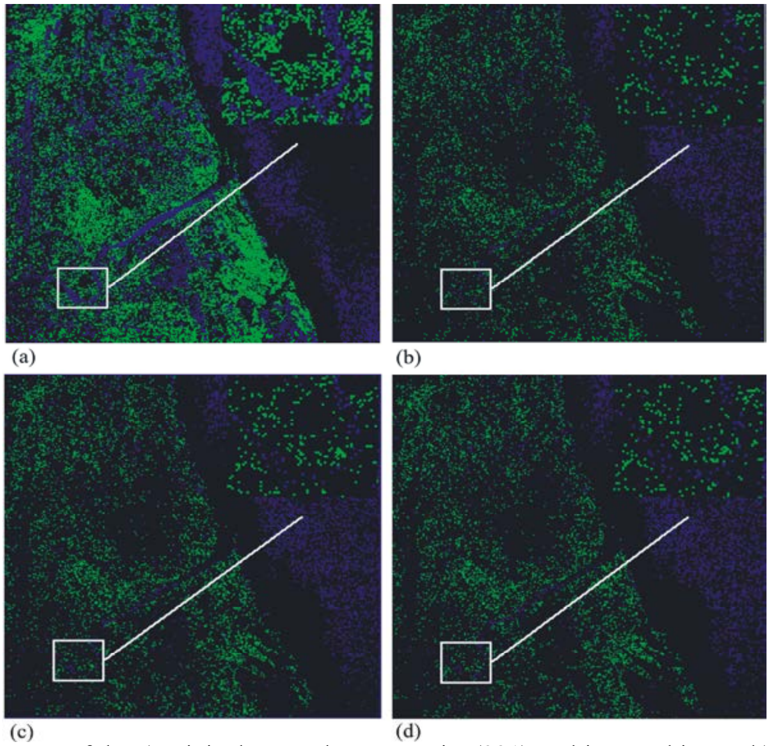

Fig. 6: Classification output of the a) original true color composite (321) multispectral image b) image compressed by haar (K=0.8298) c) image compressed by bior22 (K=0.8298) d) d) image compressed by rbio1.3 (K=0.8288)

bands is classified by using one of the unsupervised techniques; k- means algorithm with two classes namely water body and non water body. The classification output for input (true color composite) image, the image compressed with decomposition level 3 by Haar (high Kappa coefficient), bior 2.2 (medium Kappa coefficient) and rbio1.3 (low Kappa coefficient) wavelet are as shown in Fig. 6. From the classification output images, it is cleared that, even the haar produces high kappa coefficient, the bior 2.2 preserves detail information (waterbody region and its border) which results in better classification accuracy. Hence bior2.2 with decomposition level 3 is chosen as optimum for compressing three composite bands with high compression ratio, better PSNR and MSSIM also usefulness of reconstructed image for classification.

CONCLUSION

In this work, different wavelet based- multispectral band compression is presented. The impacts of wavelet basis functions, decomposition level and wavelet properties to image compression are examined. The optimum wavelet and decomposition level are selected depending upon compression ratio, reconstructed image quality (PSNR & MSSIM), Kappa coefficient and usefulness of reconstructed image for analysis and classification. From the simulation results, bior2.2 with decomposition level 3 is chosen as optimum for compressing three composite bands namely true color composite, false color composite and short wave composite band of multispectral images. However, the wavelet fails to preserve edge information in all directions. The future work will focus on image compression using multidirectional wavelet transform to be used for preserving geometric features of multispectral band imagery in all directions.

REFERENCES

1. Qian Du and James E. Fowler, 2007. Hyperspectral image compression using JPEG2000 and principal component analysis, IEEE Geoscience and Remote Sensing Letters, 4(2): 201-205.
2. Raid, A.M., W.M. Khedr, M.A. El-Dosuky and Wesam Ahmed, 2014. Image Compression Using Embedded Zerotree Wavelet.Signal & Image Processing: An International Journal (SIPIJ), 5(6): 33-39.

3. Rao, R.K. and P. Yip, 1990. NY, Discrete Cosine Transform: Algorithms, Advantages and Applications, Academic.
4. Cagnazzo Marco, Giovanni Poggi and Luisa Verdoliva, 2007. Region-Based Transform Coding of Multispectral Images, IEEE Transactions on Image Processing.
5. Buccigrossi, R.W. and E.P. Simoncelli, 1999. Image Compression via Joint Statistical Characterization in the Wavelet Domain, IEEE Transactions on Image Processing, 8(1): 1688-1700.
6. DeVore, R.A., B. Jawerth and B.J. Lucier, 1992. Image compression through wavelet transforms coding, IEEE Transactions on Information Theory, 38(2): 719-746.
7. Strang, G. and T. Nguyen, 1996. Wavelets and Filter Banks, Cambridge Press.
8. Amato, F., C. Galdi and G. Poggi, 1997. Embedded zerotree wavelet coding of multispectral images. Proc. IEEE Int. Conf. Image Processing, Santa Barbara, CA, pp: 612-616.
9. Vaisey, J., M. Barlaud and M. Antonini, 1998. Multispectral image coding using lattice VQ and the wavelet transform. Proc. IEEE Int. Conf. Image Processing, Chicago, IL, pp: 307-311.
10. Dragotti, P.L., G. Poggi and A.R.P. Ragozini, 2000. Compression of multispectral images by three-dimensional SPIHT algorithm, IEEE Trans.Geosci. Remote Sens., 38(1): 416-428.
11. Fowler, J.E. and D.N. Fox, 2001. Embedded wavelet-based coding of threedimensional oceanographic images with land masses. IEEE Trans.Geosci. Remote Sensing, 39(1): 284-290.
12. Wang, Y., J.T. Rucker and J.E. Fowler, 2004. Three-dimensional tarp coding for the compression of hyperspectral images, IEEE Geosci. Remote Sens. Lett., 42(4): 136-140.
13. Penna, B., T. Tillo, E. Magli and G. Olmo, 2006. Progressive 3-D coding of hyperspectral images based on JPEG 2000, IEEE Geosci. RemoteSens. Lett., 44(1): 125-129.
14. Penna, B., T. Tillo, E. Magli and G. Olmo, 2007. Transform coding techniques for lossy hyperspectral data compression, IEEE Geosci. Remote Sens. Letters, 45(5): 1408-1421.
15. Grgic Sonja, Mislav Grgic and Branka Zovko-Cihlar, 2001. Performance Analysis of Image Compression Using Wavelets, IEEE Trans. On Industrial Electronics, 48(3): 682-695.
16. Kale, Vinay U. and Nikkoo N. Khalsa, 2010. Performance Evaluation of Various Wavelets for Image Compression of Natural and Artificial Images, International Journal of Computer Science & Communication, 1(1): 179-184.
17. Singh Tripatjot, 2011. Performance and Comparative Analysis of Still Image for Compression Ratio using Wavelets, International Journal of Electronics and Communication Engineering, 4(3): 275-282.
18. Sridhar, S., P. Rajesh Kumar and K.V. Ramanaiah, 2014. Wavelet Transform Techniques for Image Compression-An Evaluation. International Journal of Image, Graphics and Signal Processing, 2(1): 54-67.
19. Pandey Vikas, 2014. Analysis of Image Compression using Wavelets, International Journal of Computer Applications, 103(17): 1-8.
20. Shukla Monika, Sonika Arrora and Mangal Singh, 2013. Image Compression Using Wavelet Family on Biomedical Application (ultra sound), International Journal of Advanced Research in Computer Science and Software Engineering, 3(8): 946-950.
21. Kousalyadevi, R. and S.S. Ramakrishnan, 2012. Performance Analysis of Multi Spectral Band Image Compression using Discrete Wavelet Transform, Journal of Computer Science, 8(5): 789-795.
22. Kousalyadevi, R. and S.S. Ramakrishnan, 2012. Multispectral Band Image Compression Using Wavelets, International Journal of Current Research, 4(7): 99-103.
23. Merry, R.J.E., 2005. Wavelet Theory and Applications - A literature study. Eindhoven University of Technology, DCT, pp: 53.